A computational study of intrinsic and extrinsic defects in $LiNbO_3$

2007 J. Phys.: Condens. Matter 19 046211

(http://iopscience.iop.org/0953-8984/19/4/046211)

INSTITUTE OF PHYSICS PUBLISHING JOURNAL OF PHYSICS: CONDENSED MATTER

J. Phys.: Condens. Matter **19** (2007) 046211 (10pp) doi:10.1088/0953-8984/19/4/046211

A computational study of intrinsic and extrinsic defects in $LiNbO_3$

Romel M Araujo[1], Krisztián Lengyel[2], Robert A Jackson[3,4], László Kovács[2] and Mário E G Valerio[1]

[1] Physics Department, Federal University of Sergipe, Campus Universitario, 49100-000 São Cristovão, SE, Brazil
[2] Research Institute for Solid State Physics and Optics, Hungarian Academy of Sciences, Konkoly-Thege M. út 29-33, 1121 Budapest, Hungary
[3] Lennard-Jones Laboratories, School of Physical and Geographical Sciences, Keele University, Keele, Staffordshire ST5 5BG, UK

E-mail: raraujo@fisica.ufs.br, klengyel@mail.szfki.hu, r.a.jackson@chem.keele.ac.uk, lkovacs@mail.szfki.hu and mvalerio@fisica.ufs.br

Received 20 July 2006, in final form 27 November 2006
Published 12 January 2007
Online at stacks.iop.org/JPhysCM/19/046211

Abstract

Lithium niobate is a material with many important technological applications as a result of its diverse physical properties. Using a recently derived interatomic potential, intrinsic defect energies have been calculated leading to conclusions about the defect properties of the material that are compared with experimental conclusions. The incorporation of dopant ions into the structure is also considered, and solution energies are calculated, which enable predictions to be made about which ions are most easily added and which solution energy schemes are favoured energetically.

1. Introduction

Lithium niobate is a material of great technological importance, with many applications in devices that exploit its properties, ranging from elastic to photorefractive [1–4]. Intrinsic defects due to non-stoichiometry strongly influence the properties of $LiNbO_3$ crystals; therefore a clear understanding of their structure is essential. Several models have been deduced for the defects from the data reported in hundreds of experimental papers [2–5], but relatively few computational studies of the possible defect structures have been published so far [6–10]. The computer-simulation studies of Donnerberg *et al* [7] have shown that the important defects are $(Nb_{Li}^{\bullet\bullet\bullet\bullet}V_{Nb}^{\prime\prime\prime\prime\prime})^{\prime}$ and isolated $Nb_{Li}^{\bullet\bullet\bullet\bullet}$ antisites. Although the former defect is energetically less favourable the contradiction was resolved by assuming the existence of an ilmenite-like stacking sequence in $LiNbO_3$ [11]. In a recently published paper [12] a new interatomic

[4] Author to whom any correspondence should be addressed.

potential was reported for this material, which reproduced the properties of the ferroelectric and paraelectric phases of the material and which gave a generally better level of agreement with experiment than that obtained by the earlier potential due to Donnerberg and co-workers [6–10]. In this paper the new potential is employed in a survey of intrinsic and extrinsic defects in $LiNbO_3$, extending the calculations of defect formation energies to interstitials and defect complexes such as $(Nb_{Li}^{\bullet\bullet\bullet\bullet}–4\ V'_{Li})$ and $(Nb_{Li}^{\bullet\bullet\bullet\bullet}–V''''''_{Nb})'$ clusters, and to energies of possible reactions leading to Li_2O deficiency. Extrinsic defects are then considered in a study of doping by a range of M^{2+} and M^{3+} metal cations.

2. Computational background

The application of computer modelling techniques to the study of the defect chemistry of solid state materials is widely established; recent applications to technologically important materials have included topaz, used in dosimeter devices [13], and $LiCaAlF_6/LiSrAlF_6$ [14] and BaY_2F_8 [15], used as solid state laser materials. Use is made of the Mott–Littleton method [16] in which point defects are considered to be at the centre of a region in which all interactions are treated explicitly, while approximate methods are employed for regions of the lattice more distant from the defect. The calculations were performed using the GULP code [17]. The potentials used were fitted to the structures of $LiNbO_3$ (ferroelectric phase, [18]), Li_2O and Nb_2O_5, using the free energy minimization option, at a temperature of 293 K (see [12] for full details of the procedure used). The potentials for the dopant ion–oxygen interactions were obtained by fitting to the parent oxide structures, and are given in table 5.

3. Intrinsic defects in $LiNbO_3$

In this section, defect formation energies are reported that were calculated for the ferroelectric phase of the material, optimized using the new potential, which is reported in [12], along with details of the agreement between calculated and experimentally determined structures and lattice properties.

3.1. Defect formation energies

In table 1, intrinsic defect formation energies for $LiNbO_3$ are given, assuming one interstitial site at (0.0, 0.0, 0.139 36) which corresponds to the centre of the empty oxygen octahedron in the structure (the structural cation vacancy). The calculations have been performed at two temperatures, 0 and 293 K (the latter being the temperature employed in the potential fitting). It is stressed that these basic defect formation energies (vacancies, interstitials; table 1(a)) on their own do not have any direct significance, and that they are combined to form Frenkel, Schottky and pseudo-Schottky defect formation energies (table 1(b)). The lattice energies used are also given (table 1(c)). The corresponding values obtained by Donnerberg *et al* [7] are also given in the table. Agreement between raw defect formation energies calculated using different potentials is not expected, but the trends in Frenkel, Schottky and pseudo-Schottky defect formation energies should agree, as is observed. From this table it is seen that the most likely defects to occur are Li^+ Frenkel defects (vacancies and interstitials), but Li_2O pseudo-Schottky disorder (Li^+ and O^{2-} vacancies) may also occur. However, these conclusions do not take into account the observed lithium deficiency in the material, and more complex defect models are required, as considered in the next section.

Table 1. Intrinsic defect formation energies.

	Formation energy per defect (eV)		
	This work		
Defect	0 K	293 K	Reference [7]
(a) Basic defect formation energies (eV)			
V'_{Li}	9.81	9.71	9.8
V''''_{Nb}	127.56	127.45	117.3
$V^{\bullet\bullet}_{O}$	18.98	18.91	19.5
$Li^{\bullet}_{i}$	−7.08	−7.12	
$Nb^{\bullet\bullet\bullet\bullet\bullet}_{i}$	−104.12	−104.25	
O''_{i}	−9.47	−9.64	
$Nb^{\bullet\bullet\bullet\bullet}_{Li}$	−98.37	−98.49	−99.5
(b) Frenkel, Schottky and pseudo-Schottky defect formation energies (eV) (based on unbound defects)			
Li Frenkel	1.37	1.30	0.93
Nb Frenkel	11.72	11.60	6.26
O Frenkel	4.76	4.64	3.42
Schottky $LiNbO_3$	3.95	3.85	3.91
Pseudo-Schottky Li_2O	1.81	1.80	1.94
Pseudo-Schottky Nb_2O_5	5.09	5.07	2.85
(c) Lattice energies (eV)			
$LiNbO_3$	−174.57	−174.66	
Li_2O	−33.16	−32.92	
Nb_2O_5	−314.37	−313.99	

3.2. Defect reactions

The lithium deficiency/niobium excess in $LiNbO_3$ can be explained in several ways. Historically, three models were proposed [19], which explained the non-stoichiometry in different ways:

(1) Lithium vacancies compensated by oxygen vacancies.
(2) Niobium interstitials compensated by oxygen interstitials.
(3) Antisite or interstitial niobium compensated by lithium or niobium vacancies.

The three models were tested by calculating the expected density of the crystal as a function of the Li/Nb ratio, and experimentally determined densities agreed with the predictions of model 3, ruling out the first two [20]. Subsequently, further support for this model came from x-ray and neutron diffraction measurements [21] and NMR measurements [22].

Based on model 3, three defect reactions are considered in this paper.

(i) Antisite niobium compensated by lithium vacancies
In this reaction, a Nb^{5+} ion occupies a Li^{+} position, and the charge is compensated for by the creation of four Li^{+} vacancies. It can be represented by the following reaction:

$$5LiNbO_3 + \tfrac{1}{2}Nb_2O_5 \rightarrow 5(V'_{Li})_{4/5}(Nb^{\bullet\bullet\bullet\bullet}_{Li})_{1/5}NbO_3 + \tfrac{5}{2}Li_2O.$$

This reaction can also be written in the form used in [14]:

$$5Li_{Li} + \tfrac{1}{2}Nb_2O_5 \rightarrow 4V'_{Li} + Nb^{\bullet\bullet\bullet\bullet}_{Li} + \tfrac{5}{2}Li_2O.$$

Table 2. Energies of possible reactions that lead to Li_2O deficiency (calculated using 293 K defect formation energies from table 1).

Model	Formation energy per Li_2O unit (eV)
Antisite Nb compensated by Li vacancies	3.01 (2.24[a])
Antisite Nb compensated by Nb vacancies	36.82
Interstitial Nb compensated by Li vacancies	7.60

[a] Calculated including binding energy for the defect cluster.

(ii) Antisite niobium compensated by niobium vacancies
In this reaction, charge compensation for five Nb^{5+} ions substituted at Li^+ sites is provided by four Nb^{5+} vacancies, and it is represented as follows:

$$5LiNbO_3 + \tfrac{1}{2}Nb_2O_5 \rightarrow 5Nb_{Li}^{\bullet\bullet\bullet\bullet}(V_{Nb}^{\prime\prime\prime\prime\prime})_{4/5}Nb_{1/5}O_3 + \tfrac{5}{2}Li_2O.$$

In alternative form this reaction may be written:

$$5Li_{Li} + 4Nb_{Nb} + \tfrac{1}{2}Nb_2O_5 \rightarrow 5Nb_{Li}^{\bullet\bullet\bullet\bullet} + 4V_{Nb}^{\prime\prime\prime\prime\prime} + \tfrac{5}{2}Li_2O.$$

(iii) Interstitial niobium compensated by lithium vacancies
In this reaction, five Li^+ vacancies are compensated by a Nb^{5+} interstitial ion:

$$5LiNbO_3 + \tfrac{1}{2}Nb_2O_5 \rightarrow 5V_{Li}^{\prime}NbO_3 + Nb_i^{\bullet\bullet\bullet\bullet\bullet} + \tfrac{5}{2}Li_2O.$$

Or, in alternative form:

$$5Li_{Li} + \tfrac{1}{2}Nb_2O_5 \rightarrow 5V_{Li}^{\prime} + Nb_i^{\bullet\bullet\bullet\bullet\bullet} + \tfrac{5}{2}Li_2O.$$

Using the defect formation energies given in table 1, energies for these reactions have been calculated, and these are given in table 2. In addition, it is found that the defect configuration used in reaction (i), $(4V_{Li}^{\prime} + Nb_{Li}^{\bullet\bullet\bullet\bullet})$, has a small binding energy, and so the energy given in brackets takes this binding into account. No binding was observed with reactions (ii) and (iii). From the table, it can be seen that only the antisite niobium–lithium vacancy reaction is energetically feasible. The calculations therefore support the variant of model 3 with niobium antisite occupancy compensated by lithium vacancies.

4. Extrinsic defects in $LiNbO_3$

Doping of a range of divalent and trivalent cations into $LiNbO_3$ has been considered. In either case there is the possibility that the dopant ion can substitute at either the Li^+ or the Nb^{5+} site, and there is more than one possible mode of charge compensation in either situation. Divalent and trivalent ion substitution will be considered separately.

4.1. Divalent ion substitution

Four charge compensation schemes are considered, corresponding to the following reactions:

(i) $MO + 2Li_{Li} \rightarrow M_{Li}^{\bullet} + V_{Li}^{\prime} + Li_2O$
(ii) $4MO + 3Li_{Li} + Nb_{Nb} \rightarrow 3M_{Li}^{\bullet} + M_{Nb}^{\prime\prime\prime} + Li_2O + LiNbO_3$
(iii) $4MO + 4Nb_{Nb} + 3Li_{Li} \rightarrow 4M_{Nb}^{\prime\prime\prime} + 3Nb_{Li}^{\bullet\bullet\bullet\bullet} + Li_2O + LiNbO_3$
(iv) $MO + 2Li_{Li} + Nb_{Nb} \rightarrow M_{Nb}^{\prime\prime\prime} + V_{Li}^{\prime} + Nb_{Li}^{\bullet\bullet\bullet\bullet} + Li_2O.$

Defect formation energies, corresponding to the energy required to carry out the substitution plus charge compensation, have been calculated and are summarized in table 3, sections (a) and (b). In section (a), the energies have been calculated from the formation energies of the separate defects, while in section (b) they include the defect binding energy.

Table 3. Summary of substitution energies.

(a) M^{2+} dopants, unbound defects

	$M^{\bullet}_{Li}$		M'''_{Nb}		Scheme (i)		Scheme (ii)		Scheme (iii)		Scheme (iv)	
M	0 K	293 K	0 K	293 K	0 K	293 K	0 K	293 K	0 K	293 K	0 K	293 K
Mg	−15.36	−15.44	95.18	94.98	−5.55	−5.73	49.10	48.66	85.61	84.45	6.62	6.20
Mn	−12.44	−12.55	97.61	97.43	−2.63	−2.84	60.29	59.78	95.33	94.25	9.05	8.65
Fe	−13.43	−13.53	96.80	96.62	−3.62	−3.82	56.51	56.03	92.09	91.01	8.24	7.84
Co	−14.29	−14.37	96.09	95.93	−4.48	−4.66	53.22	52.82	89.25	88.25	7.53	7.15
Ni	−16.50	−16.57	94.16	93.99	−6.69	−6.86	44.66	44.28	81.53	80.49	5.60	5.21
Zn	−13.53	−13.60	96.77	96.58	−3.72	−3.89	56.18	55.78	91.97	90.85	8.21	7.80
Sr	−7.14	−7.34	101.99	101.87	2.67	2.37	80.57	79.85	112.85	112.01	13.43	13.09
Cd	−10.22	−10.35	99.43	99.25	−0.41	−0.64	68.77	68.20	102.61	101.53	10.87	10.47
Ba	−2.30	−2.54	107.70	106.37	7.51	7.17	100.80	98.75	135.69	130.01	19.14	17.59
Pb	−15.50	−15.57	95.09	94.93	−5.69	−5.86	48.59	48.22	85.25	84.25	6.53	6.15

(b) M^{2+} dopants, bound defects

	Scheme (i)		Scheme (ii)		Scheme (iii)		Scheme (iv)	
M	0 K	293 K	0 K	293 K	0 K	293 K	0 K	293 K
Mg	−6.04	−6.66	45.98	46.68	52.42	54.78	−1.98	6.20
Mn	−3.15	−3.47	57.18	57.66	62.80	69.34	0.81	8.65
Fe	−4.13	−4.45	53.37	53.92	58.47	60.09	−0.15	7.84
Co	−4.96	−5.28	50.26	50.74	56.09	62.47	−0.91	7.15
Ni	−7.17	−7.47	41.68	42.37	49.02	50.63	−2.47	5.21
Zn	−4.19	−4.52	53.23	53.59	58.55	72.96	0.28	7.80
Sr	2.03	1.65	75.91	77.15	87.82	85.80	6.40	13.09
Cd	−0.97	−1.31	64.45	65.91	71.22	71.98	3.01	10.47
Ba	6.87	6.41	96.84	94.79	104.17	105.01	11.15	17.59
Pb	−6.76	−6.47	48.13	46.20	51.83	54.62	−1.39	6.15

Defect formation energies, on their own, do not provide information on the overall energetics of the substitution process, so solution energies are calculated, which include all energy terms involved. For example, the solution energy, E_{sol}, for reaction (i) is given by:

$$E_{sol} = -E_{latt}(MO) + E(M^{\bullet}_{Li} + V'_{Li}) + E_{latt}(Li_2O)$$

where the E_{latt} terms are lattice energies, and Kroger–Vink notation is employed for the defect formation energies. The solution energies per dopant ion are given in tables 4(a) and (b), where the values in table 4(b) correspond to bound defects, where the binding energy has been taken into account.

From table 4(b) it can be seen that scheme (ii), involving doping at both sites, is the lowest energy scheme at 0 K, and at 293 K except for Fe and Cd. Scheme (iii), involving substitution at the Nb^{5+} site with charge compensation by Nb^{5+} ions at Li^{+} sites, gives the lowest energies at 293 K in these two cases. It can also be seen from tables 4(a) and (b) that there is considerable defect binding in all cases, so that the dopant and charge compensating defects are likely to be found adjacent to one another.

4.2. Trivalent ion substitution

As with divalent ion substitution, four substitution reaction schemes are considered:

Table 3. (Continued.)

(c) M^{3+} dopants, unbound defects

	$M_{Li}^{\bullet\bullet}$		M_{Nb}''		Scheme (i)		Scheme (ii)		Scheme (iii)		Scheme (iv)	
M	0 K	293 K	0 K	293 K	0 K	293 K	0 K	293 K	0 K	293 K	0 K	293 K
Ce	−28.25	−28.47	78.20	78.04	−17.26	−18.10	49.95	49.57	58.03	57.59	−1.10	−2.06
Pr	−28.61	−28.80	77.70	77.54	−17.98	−18.76	49.09	48.74	57.03	56.59	−2.10	−3.06
Nd	−28.46	−28.69	77.81	77.61	−17.68	−18.54	49.35	48.92	57.25	56.73	−1.88	−2.92
Sm	−29.92	−29.40	77.09	76.94	−20.6	−19.96	47.17	47.54	55.81	55.39	−3.32	−4.26
Eu	−29.70	−29.87	76.63	76.48	−20.16	−20.90	46.93	46.61	54.89	54.47	−4.24	−5.18
Gd	−30.14	−30.30	76.21	76.07	−21.04	−21.76	46.07	45.77	54.05	53.65	−5.08	−6.00
Tb	−30.22	−30.37	76.09	75.94	−21.2	−21.90	45.87	45.57	53.81	53.39	−5.32	−6.26
Dy	−30.93	−31.08	75.45	75.31	−22.62	−23.32	44.52	44.23	52.53	52.13	−6.60	−7.52
Ho	−31.24	−31.40	75.14	75.00	−23.24	−23.96	43.90	43.60	51.91	51.51	−7.22	−8.14
Er	−31.70	−31.85	74.72	74.58	−24.16	−24.86	43.02	42.73	51.07	50.67	−8.06	−8.98
Tm	−32.21	−32.35	74.24	74.10	−25.18	−25.86	42.03	41.75	50.11	49.71	−9.02	−9.94
Yb	−32.35	−32.48	74.11	73.97	−25.46	−26.12	41.76	41.49	49.85	49.45	−9.28	−10.20
Lu	−32.73	−32.75	73.76	73.73	−26.22	−26.66	41.03	40.98	49.15	48.97	−9.98	−10.68

(d) M^{3+} dopants, bound defects

	Scheme (i)		Scheme (ii)		Scheme (iii)		Scheme (iv)	
M	0 K	293 K	0 K	293 K	0 K	293 K	0 K	293 K
Ce	−19.11	−19.42	47.04	47.99	51.45	49.48	−17.23	−11.82
Pr	−19.89	−20.20	46.18	47.12	50.23	44.35	−13.24	−14.16
Nd	−19.61	−19.99	46.36	47.30	50.37	47.21	−18.34	−14.04
Sm	−21.05	−21.45	44.96	45.91	49.38	42.21	−19.45	−17.58
Eu	−22.01	−22.96	44.86	44.98	48.03	45.07	−16.31	−14.13
Gd	−22.88	−23.92	44.08	44.14	45.57	40.12	−16.15	−16.51
Tb	−23.03	−24.57	42.99	43.97	45.86	39.02	−20.25	−16.54
Dy	−24.47	−25.70	41.89	42.61	45.57	37.48	−23.50	−16.13
Ho	−25.09	−26.41	41.03	42.01	44.95	37.27	−19.37	−18.33
Er	−26.07	−27.35	41.61	41.15	44.20	34.73	−20.54	−17.51
Tm	−27.07	−28.71	40.09	40.22	42.97	36.41	−21.26	−20.13
Yb	−27.26	−28.73	39.21	39.96	42.80	35.80	−26.15	−20.59
Lu	−27.80	−29.51	38.45	39.47	42.29	34.30	−26.28	−20.49

(i) $M_2O_3 + 6Li_{Li} \rightarrow 2M_{Li}^{\bullet\bullet} + 4V_{Li}' + 3Li_2O$
(ii) $M_2O_3 + Li_{Li} + Nb_{Nb} \rightarrow M_{Li}^{\bullet\bullet} + M_{Nb}'' + LiNbO_3$
(iii) $M_2O_3 + Li_{Li} + 2Nb_{Nb} \rightarrow 2M_{Nb}'' + Nb_{Li}^{\bullet\bullet\bullet\bullet} + LiNbO_3$
(iv) $M_2O_3 + 6Li_{Li} + 2Nb_{Nb} \rightarrow 2M_{Nb}'' + 4V_{Li}' + 2Nb_{Li}^{\bullet\bullet\bullet\bullet} + 3Li_2O.$

Defect formation energies, with and without defect binding, are summarized in tables 3(c) and (d), and the corresponding solution energies per dopant ion are given in tables 4(c) and (d).

From the table it can be seen that the preferred scheme for all dopants at 0 K is scheme (ii) with co-doping at both the Li^+ and Nb^{5+} sites, but that at 293 K scheme (iii) becomes very favourable, with substitution at the Nb^{5+} site with antisite Nb compensation, with the exception of Ce and Eu, which prefer scheme (ii). As with the divalent dopants, it can be seen, comparing tables 4(c) and (d), that there is considerable binding, again leading to the conclusion that the dopant ion and charge compensating defect will be located in neighbouring sites. These observations are confirmed by figure 1, in which the solution energies for all four

Table 4. Summary of solution energies.

(a) M^{2+} dopants, unbound defects (energies per dopant ion)

	Scheme (i)		Scheme (ii)		Scheme (iii)		Scheme (iv)	
M	0 K	293 K	0 K	293 K	0 K	293 K	0 K	293 K
Mg	2.33	2.29	1.38	1.21	10.51	10.16	14.50	14.22
Mn	2.53	2.52	1.46	1.33	10.22	9.95	14.21	14.01
Fe	2.43	2.43	1.41	1.28	10.30	10.03	14.29	14.09
Co	2.36	2.39	1.37	1.28	10.38	10.14	14.37	14.20
Ni	2.31	2.29	1.39	1.25	10.61	10.30	14.60	14.36
Zn	2.41	2.48	1.40	1.34	10.35	10.11	14.34	14.17
Sr	4.01	3.93	2.71	2.55	10.78	10.59	14.77	14.65
Cd	2.96	2.97	1.79	1.69	10.25	10.02	14.24	14.08
Ba	5.64	6.20	4.56	4.74	13.28	12.56	17.27	16.62
Pb	1.50	1.59	0.57	0.53	9.73	9.54	13.72	13.60

(b) M^{2+} dopants, bound defects (energies per dopant ion)

	Scheme (i)		Scheme (ii)		Scheme (iii)		Scheme (iv)	
M	0 K	293 K	0 K	293 K	0 K	293 K	0 K	293 K
Mg	1.84	1.36	0.60	0.71	2.21	2.74	5.90	12.59
Mn	2.01	1.89	0.68	0.80	2.09	1.97	5.97	10.95
Fe	1.92	1.80	0.62	0.76	1.90	0.55	5.90	12.48
Co	1.88	1.77	0.63	0.76	2.09	1.94	5.93	12.52
Ni	1.83	1.68	0.65	0.77	2.48	1.08	6.53	12.46
Zn	1.94	1.85	0.66	0.79	2.00	3.89	6.41	12.32
Sr	3.37	3.21	1.55	1.87	4.52	2.28	7.74	6.58
Cd	2.40	2.30	0.71	1.11	2.40	0.88	6.38	8.76
Ba	5.00	5.44	3.57	3.75	5.40	4.56	9.28	10.87
Pb	0.43	0.98	0.45	0.02	1.38	0.38	5.80	11.29

(c) M^{3+} dopants, unbound defects (energies per dopant ion)

	Scheme (i)		Scheme (ii)		Scheme (iii)		Scheme (iv)	
M	0 K	293 K	0 K	293 K	0 K	293 K	0 K	293 K
Ce	6.25	6.15	2.31	2.04	6.35	6.05	14.33	14.17
Pr	6.29	6.20	2.28	2.00	6.25	5.92	14.23	14.05
Nd	6.36	6.23	2.33	2.01	6.29	5.91	14.27	14.04
Sm	5.86	6.53	2.19	2.33	6.52	6.25	14.50	14.38
Eu	6.48	6.45	2.47	2.25	6.46	6.18	14.44	14.31
Gd	6.40	6.38	2.41	2.20	6.40	6.13	14.38	14.26
Tb	6.43	6.42	2.42	2.21	6.39	6.12	14.37	14.25
Dy	6.14	6.12	2.17	1.95	6.17	5.90	14.15	14.02
Ho	6.26	6.24	2.28	2.07	6.29	6.02	14.27	14.15
Er	6.19	6.18	2.23	2.02	6.26	5.99	14.24	14.12
Tm	6.13	6.13	2.19	1.98	6.22	5.96	14.21	14.09
Yb	6.11	6.13	2.18	1.98	6.22	5.96	14.20	14.09
Lu	5.96	6.08	2.04	1.95	6.10	5.94	14.08	14.07

schemes were plotted as function of the ionic radii of the RE^{3+} ions. The ionic radii were taken from [23] for RE^{3+} ions in six-fold coordination. Figure 1(a) presents the energy dependence at 0 K, and it can be seen that scheme (ii) has the lowest energy and that the difference between these energies and the ones from scheme (iii) are approximately constant throughout the whole

Table 4. (Continued.)

(d) M^{3+} dopants, bound defects (energies per dopant ion)								
	Scheme (i)		Scheme (ii)		Scheme (iii)		Scheme (iv)	
M	0 K	293 K	0 K	293 K	0 K	293 K	0 K	293 K
Ce	5.32	5.49	0.85	1.25	3.06	1.99	6.26	9.29
Pr	5.34	5.47	0.83	1.19	2.85	−0.20	8.66	8.50
Nd	5.40	5.50	0.84	1.20	2.85	1.15	6.04	8.48
Sm	5.63	5.78	1.09	1.51	3.30	−0.34	6.43	7.72
Eu	5.55	5.42	1.44	1.44	3.03	1.48	8.40	9.83
Gd	5.48	5.30	1.41	1.38	2.16	−0.63	8.85	9.01
Tb	5.51	5.09	0.98	1.41	2.41	−1.07	6.90	9.11
Dy	5.22	4.93	0.85	1.14	2.69	−1.43	5.70	9.72
Ho	5.33	5.01	0.84	1.27	2.81	−1.10	8.19	9.05
Er	5.23	4.94	1.53	1.24	2.82	−1.98	8.00	9.85
Tm	5.18	4.70	1.22	1.22	2.66	−0.69	8.09	8.99
Yb	5.21	4.82	0.90	1.22	2.69	−0.86	5.77	8.89
Lu	5.17	4.65	0.75	1.19	2.67	−1.40	5.93	9.16

Table 5. Potentials and lattice energies used for MO and M_2O_3 calculations.

				Lattice energy (eV)	
M	A (eV)	ρ (Å)	C (eV Å^6)	0 K	293 K
Mg	1 310.98	0.2997	0.0	−41.04	−40.94
Mn	722.30	0.3464	0.0	−38.32	−38.28
Fe	722.20	0.3399	0.0	−39.21	−39.17
Co	784.42	0.3301	0.0	−40.00	−39.97
Ni	2 694.98	0.2670	2.198	−42.16	−42.07
Zn	515.70	0.3581	0.0	−39.29	−39.29
Sr	2 309.30	0.3220	0.0	−34.50	−34.48
Cd	876.60	0.3500	0.0	−36.53	−36.53
Ba	1 819.70	0.3549	0.0	−31.92	−31.95
Pb	998.94	0.3107	0.0	−40.35	−40.37
Ce	2 803.18	0.3289	27.55	−129.32	−129.16
Pr	2 091.95	0.3399	20.34	−130.04	−129.91
Nd	1 989.20	0.3430	22.59	−128.89	−129.75
Sm	1 950.65	0.3414	21.49	−131.79	−131.77
Eu	1 924.71	0.3403	20.59	−132.59	−132.55
Gd	1 881.95	0.3399	20.34	−133.32	−133.28
Tb	1 664.28	0.3457	20.34	−133.53	−133.51
Dy	1 782.15	0.3399	20.34	−134.38	−134.32
Ho	1 744.25	0.3399	20.34	−135.23	−135.19
Er	1 707.41	0.3389	17.55	−136.01	−135.98
Tm	1 635.85	0.3399	20.34	−136.91	−136.87
Yb	1 638.25	0.3386	16.57	−137.16	−137.13
Lu	1 630.35	0.3385	19.27	−137.62	−137.57
O	22 764.0	0.149	27.88		

RE^{3+} series. On the other hand, at 293 K (figure 1(b)), there is a clear trend that as the ionic radii increase, the energies from scheme (ii) and (iii) become closer, meaning that the chance of finding both defect types increases. For the biggest RE^{3+} ion, Ce^{3+}, the lowest solution energy corresponds to scheme (iii).

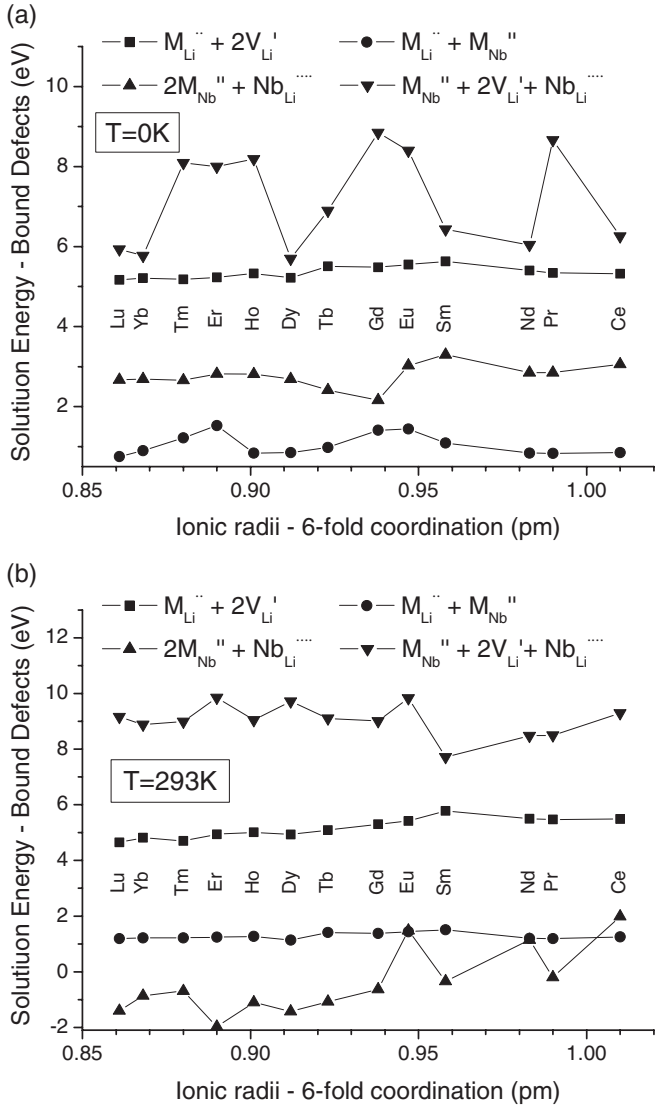

Figure 1. Solution energies for trivalent dopant ions as a function of ionic radius.

In a recently published paper [24], x-ray absorption near-edge structure techniques have been used to study both the charge and location of Fe ions in $LiNbO_3$. The paper notes that Fe is found in the +3 charge state, and that the Fe^{3+} ions are located at the Li^+ sites. A further paper which considers doping by Fe^{3+} and other transition metal ions has been recently submitted [25].

5. Conclusions

This paper has reported the application of a newly derived potential to the calculation of intrinsic and extrinsic defect formation energies in $LiNbO_3$. Basic defect formation energies

and Frenkel and Schottky energies are reported, and used to calculate the energies of defect reactions, which give rise to the experimentally observed lithium deficiency in the material. Of these reactions, the formation of antisite niobium ions compensated by lithium vacancies is found to have the lowest energy, and this is therefore the predicted intrinsic defect model. Doping of a range of M^{2+} and M^{3+} ions into the material is considered, and predictions are made of the lowest energy sites for occupation, and the corresponding charge compensation schemes.

Acknowledgments

The authors are grateful to CNPq, FAP-SE, CAPES, the British Council, the Hungarian Research and Technology Innovation Fund and the Hungarian Scientific Research Fund (OTKA No T47265) for financial support.

References

[1] Jazbinšek M and Zgonik M 2002 *Appl. Phys.* B **74** 407
[2] Räuber A 1978 *Current Topics in Materials Science* vol 1, ed E Kaldis (Amsterdam: North-Holland) p 481
[3] Prokhorov A M and Kuz'minov Yu S 1990 *Physics and Chemistry of Crystalline Lithium Niobate* 1st edn (New York: Hilger)
[4] Wong K K (ed) 2004 *Properties of Lithium Niobate* (London: IEE)
[5] Schirmer O F, Thiemann O and Wöhlecke M 1991 *J. Phys. Chem. Solids* **52** 185
[6] Tomlinson S M, Freeman C M, Catlow C R A, Donnerberg H and Leslie M 1989 *J. Chem. Soc. Faraday Trans.* 2 **85** 367
[7] Donnerberg H, Tomlinson S M, Catlow C R A and Schirmer O F 1989 *Phys. Rev.* B **40** 11909
[8] Tomlinson S M, Catlow C R A, Donnerberg H and Leslie M 1990 *Mol. Simul.* **4** 335
[9] Donnerberg H, Tomlinson S M and Catlow C R A 1991 *J. Phys. Chem. Solids* **52** 201
[10] Donnerberg H 1999 *Atomic Simulations of Electrooptic and Magnetooptic Oxide Materials* (*Springer Series 'Transactions in Modern Physics'*) (Berlin: Springer)
[11] Smyth D M 1986 *Proc. 6th IEEE Int. Symp. on Applications of Ferroelectrics* p 115
[12] Jackson R A and Valerio M E G 2005 *J. Phys.: Condens. Matter* **17** 837
[13] Jackson R A and Valerio M E G 2004 *J. Phys.: Condens. Matter* **16** S2771
[14] Amaral J B, Plant D F, Valerio M E G and Jackson R A 2003 *J. Phys.: Condens. Matter* **15** 2523
[15] Jackson R A, Valerio M E G, Couto dos Santos M A and Amaral J B 2005 *Phys. Status Solidi* c **2** 476
[16] Mott N F and Littleton M J 1938 *Trans. Faraday. Soc.* **34** 485
[17] Gale J D 1997 *J. Chem. Soc. Faraday Trans.* **93** 629
[18] Abrahams S C and Marsh P 1986 *Acta Crystallogr.* B **42** 61
[19] Lerner P, Legras C and Dumas J P 1968 *J. Cryst. Growth* **3/4** 231
[20] Kovács L and Polgár K 1986 *Cryst. Res. Technol.* **21** K101
[21] Iyi N, Kitamura K, Izumi F, Yamamoto J K, Hayashi T, Asano H and Kimura S 1992 *J. Solid State Chem.* **101** 340
[22] Blümel J, Born E and Metzger Th 1994 *J. Phys. Chem. Solids* **55** 589
[23] Shannon R D 1976 *Acta Crystallogr.* A **32** 751
[24] Olimov Kh, Falk M, Buse K, Woike Th, Hormes J and Modrow H 2006 *J. Phys.: Condens. Matter* **18** 5135
[25] Valerio M E G, Araujo R M and Jackson R A 2007 *J. Mater. Sci.* submitted